Pergamon

Int. J. Heat Mass Transfer. Vol. 40, No. 18, pp. 4461–4472, 1997

Printed in Great Britain
0017–9310/97 $17.00+0.00

PII: S0017–9310(97)00052–5

An aquifer–well thermal and fluid dynamic model for downhole heat exchangers with a natural convection promoter

A. CAROTENUTO,† C. CASAROSA,‡ M. DELL'ISOLA† and L. MARTORANO‡

†Dipartimento di Ingegneria Industriale, Università di Cassino, Italy
‡Dipartimento di Energetica, Università di Pisa, Italy

(*Received* 3 *October* 1996 *and in final form* 14 *January* 1997)

Abstract—Downhole heat exchangers (DHE) eliminate the problem of geothermal fluid disposal, since only heat is taken from the well. For this reason, as well as their low cost and simple installation, they are frequently used in geothermal plants. In the last few years DHEs have been provided with a natural convection promoter to improve the heat and mass transfer of geothermal fluid between the aquifer and the well. Knowledge of the interaction between the fluid in the aquifer, in the well and in the promoter is necessary for DHE design. The authors experimentally verified the existence of a limit in the heat flow obtained by the DHE, which is connected only to the aquifer–well–promoter interaction. This heat flow limit is due to the short-circuit effect in the aquifer between cold and warm fluids, respectively leaving and entering the well. The authors propose a simplified model developed to determine the main lumped parameters characterizing the heat and mass transfer between aquifer, well and natural convection promoter. © 1997 Elsevier Science.

DOWNHOLE EXCHANGERS

Downhole exchangers (DHE) are specific heat exchangers for exploiting low and medium temperature (60 and 150°C) geothermal reservoirs. In general these devices are set up by locating a coil or a simple U-tube in the geothermal well, through which the fluid of the thermal plant, generally water, circulates [1–6]. Consequently DHEs enable heat transfer without aquifer fluid being extracted from the ground below. The main advantages of these devices compared with geothermal conventional plants are the absence of: (i) pumps that operate in very corrosive geothermal fluids; and (ii) the second well to reinject the geothermal fluid after its exploitation to avoid impoverishment of the aquifer.

DHEs give rise to a number of inconveniences principally connected to the absence of fluid extraction induced flow, as result of which the heat flow rate that can be extracted from the well is tied only to the natural heat flow that occurs in the aquifer–well system. For low aquifer permeability, this flow can be particularly weak and consequently the heat flow withdrawn proves to be very limited; however, even in favourable conditions, that is for hydraulic conductivities greater than 5×10^{-4} m s^{-1} (permeability of approximately 50 darcies), DHEs are suitable systems for applications of moderate potential [3].

To improve the natural mass transfer between aquifer and well, over the last years the use of a natural convection promoter for DHE has spread [7, 8]. In particular, the natural convection promoter comprises a simple pipe, that constitutes an external shell for the DHE and extends itself for almost the entire length of the well (Fig. 1). The length of the promoter is, however, less than that of the well, so that two communicating sections are formed, a lower and an upper one. The geothermal fluid circulating in the external anulus communicates with the fluid inside the pipe

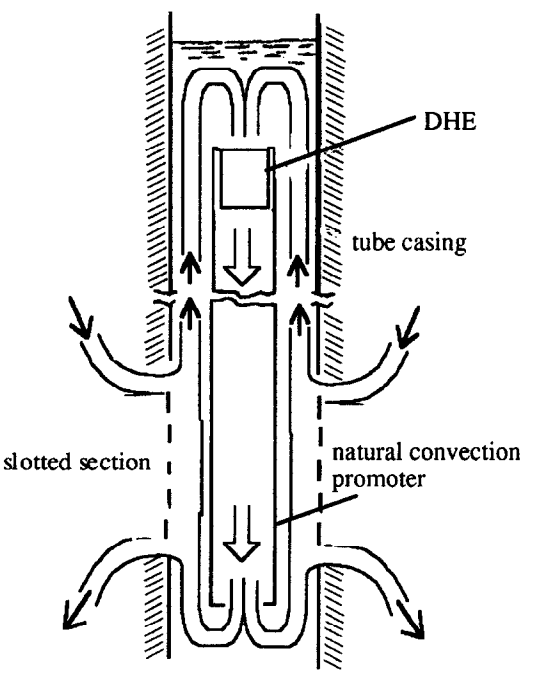

Fig. 1. Scheme of the natural convection promoter.

NOMENCLATURE

c_p	specific heat at constant pressure [kJ kg^{-1} °C^{-1}]
g	acceleration of gravity [m s^{-2}]
H	geothermal aquifer thickness [m]
h	height of the slotted section [m]
K	hydraulic conductivity [m s^{-1}]
$\dot{Q}$	heat flow rate [kW]
r	radius [m]
R	unperturbed aquifer radius [m]
T	temperature [°C]
T^*	dimensionless temperature
$\dot{m}$	mass flow-rate [kg h^{-1}]
z	vertical coordinate [m].

Greek symbols

μ	dynamic viscosity [Pa s]
β	volumetric thermal expansion coefficient [°C^{-1}]
γ	reference temperature difference [°C]
δ	circulation ratio
ζ	dimensionless length
λ_{eq}	equivalent thermal conductivity [W m^{-1} °C^{-1}]
ξ	dimensionless parameter defined by equation (40)
ρ	density [kg m^{-3}]
τ	parameter defined by equation (11) [W °C^{-1}]
χ	dimensionless parameter defined by equation (40)
ψ	stream function [m^2 s^{-1}].

Superscripts and subscripts

a	aquifer
c	condenser
e	evaporator
f	geothermal fluid in the well
i	input
l	liquid phase
m	average
max	maximum
o	output
s	impermeable stratum
w	well
∞	unperturbed aquifer.

by means of these communicating sections. The fluid circulating in the external anulus is at a higher temperature compared to the internal fluid since the latter is cooled by the DHE. The difference in density between the two columns of water supplies the driving force necessary for circulating the geothermal fluid entering and exiting the promoter, thereby contrasting the formation of a strong temperature gradient along the well axis and assuring natural convection between the geothermal fluid and the external surface of the DHE. This circulation should also improve the exchange in geothermal fluid between the aquifer and the well, thereby providing favourable conditions for geothermal energy extraction [7, 8].

A particular type of DHE is the geothermal convector (GTC), which is a special geothermal application of the two-phase thermosyphon. It consists of a sealed vessel (usually a simple vertical tube) partially filled with a working fluid (usually a refrigerant fluid). At the bottom the working fluid evaporates, the vapour rises to the top where it condenses and it transfers heat flow to the fluid of the user plant, then the condensate returns by gravity to the evaporator section. Thus, heat transfer occurs by phase change with negligible thermal gradients. In geothermal applications the two-phase thermosyphon works with a evaporator downhole and with a condenser at the ground level. GTC use to extract heat from geothermal aquifers was proposed some years ago by the authors and at the beginning of the 1980s a first prototype was designed, constructed and installed in the geothermal area of Naples [9, 10]. On the basis of this first experience, in the following years research was carried out to understand the problems that the device gave in this type of application [11] and to identify solutions to them [12]. In the 1990s, on the basis of experience gained a new GTC prototype, termed 'second generation', was designed and set up [12].

The second generation GTC was tested experimentally for a long time between 1989 and 1994 in a specially set up well in a geothermal aquifer on the island of Ischia with a geothermal fluid temperature in unperturbed conditions, T_∞, of 73.3°C. The GTC prototype comprises essentially (i) a condenser, (ii) an adiabatic section connecting condenser and (iii) an evaporator tube bundle.

The second generation prototype also comprises a natural convection promoter [12].

EXPERIMENTAL RESULTS

The measurement tests carried out on the Ischia plant have produced very interesting results about (i) the working of the GTC; (ii) the thermal fluid dynamics of the geothermal fluid in the natural convection promoter; and (iii) the heat and mass transfer between the aquifer and the well [12, 13].

In this paper the authors deal with the results regarding point (iii).

The experimental results gathered during the various measurement tests carried out on the Ischia plant,

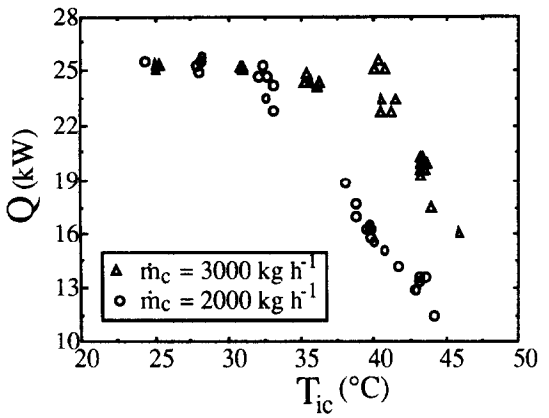

Fig. 2. Heat flow rate transferred by the Ischia GTC for variations in condenser input temperature.

showed there to be an upper limit to the heat flow rate that can be withdrawn by the GTC.

Some of the experimental results are highlighted in Figs. 2 and 3, where the heat flow rate, $\dot{Q}$, transferred by the GTC is shown as the mass flow rate $\dot{m}_c$ of the cooling water circulating in the condenser varies in relation to (i) the condenser input temperatures of the cooling water, T_{ic}, of the thermal plant (Fig. 2) and (ii) the geothermal fluid temperatures inlet to the evaporator, T_{ie} (Fig. 3). Figure 2 shows how, for $\dot{m}_c$ being the same, as the temperature T_{ic} diminishes, there is a corresponding increase in the heat flow rate transferred by the GTC up to a maximum value of circa 26 kW.

Once this maximum level has been reached, $\dot{Q}_{max}$ remains constant in an appreciably stable manner, independently of the decrease in condenser input temperatures T_{ic}. Consistent diminutions of T_{ic} give rise, however, to unstable operating conditions of the GTC–well–aquifer system which leads to thermal blocking of the device. Even the diagram in Fig. 3 shows the existence of this maximum heat flow rate value, $\dot{Q}_{max}$. It should be noted, however, that the geothermal thermal fluid temperature on entering the evaporator tube bundle, T_{ie}, continues to diminish even when the maximum value of heat flow rate has been reached. This phenomenon induced the authors to believe that the existence of this maximum is exclusively connected to the heat and mass transfer of the geothermal fluid occurring between the well and the aquifer.

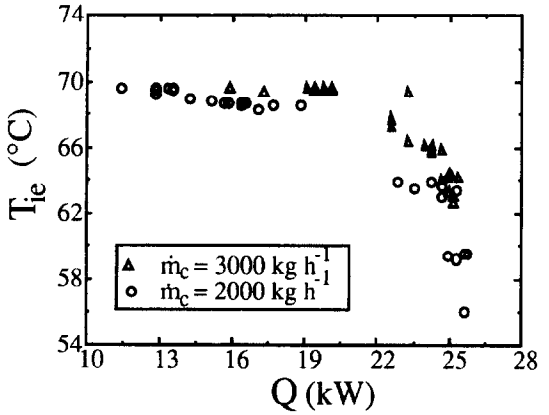

Fig. 3. Heat flow rate transferred by the Ischia GTC for variations in the input temperature of the tube bundle input geothermal fluid.

A physically plausible explanation of this phenomenon is reported in ref. [14], and is based on the concept that, near to the casing tube, the flow of the geothermal fluid short circuits as illustrated in Fig. 4(a) and (b). In this hypothesis the mean temperature of renewed fluid entering the slotted section of tube casing, T_{iw}, is not equal to the aquifer unperturbed temperature T_∞, since it transfers heat and mass to part of the well output fluid, $\dot{m}_f$, that is at a lower temperature. Thus, it follows that the temperature of the renewed fluid will depend, in fact, on the short circuit effect that occurs near the slotted section of tube casing. Consequently the mean temperature of the geothermal fluid inlet in the well is less than the unperturbed aquifer temperature, in particular, when the heat flow rate transferred by DHE increases T_{iw} diminishes.

Two fluid-dynamic limit conditions can be delineated: the first in which the mass flow rate circulating in the well, $\dot{m}_f$, is greater than the renewed mass flow rate, $\dot{m}_a$, of the aquifer [Fig. 4(a)]; and the second in which vice versa $\dot{m}_a$ is greater than $\dot{m}_f$ [Fig. 4(b)]. The hypothesis assumed in case (a) is supported by the temperature profile obtained experimentally at the Ischia well [10, 13, 14].

A simplified model with lumped parameters taking into account the short circuit phenomenon was developed by the authors in order to design a DHE with a natural convection promoter.

THE THERMAL AND FLUID DYNAMIC SIMPLIFIED MODEL OF AQUIFER–WELL–PROMOTER

With reference to Fig. 5 it is, therefore, possible to formulate the following simplified balance equations with lumped parameters. The mass balance of the renewed geothermal fluid entering into the well is given by the following equation:

$$\dot{m}_{a1} + \dot{m}_{a2} = \dot{m}_a. \tag{1}$$

Defining the short circuit ratio and the circulation ratio respectively as:

$$\sigma = \frac{\dot{m}_{a1}}{\dot{m}_{a2}} \quad \text{with } 0 \leqslant \sigma \leqslant 1 \tag{2}$$

$$\delta = \frac{\dot{m}_a}{\dot{m}_f} \tag{3}$$

equation (1) becomes

$$1 - \sigma = \frac{\dot{m}_{a2}}{\dot{m}_a}. \tag{4}$$

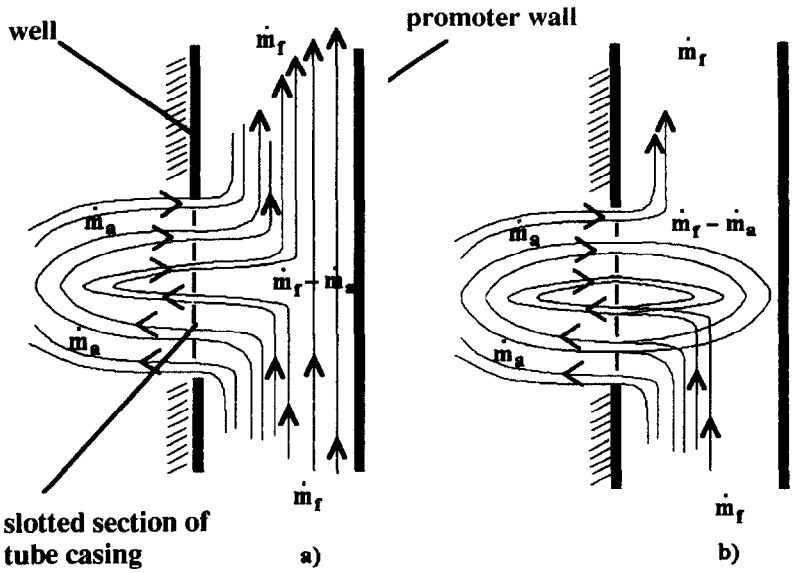

Fig. 4. Geothermal fluid flow between well and aquifer.

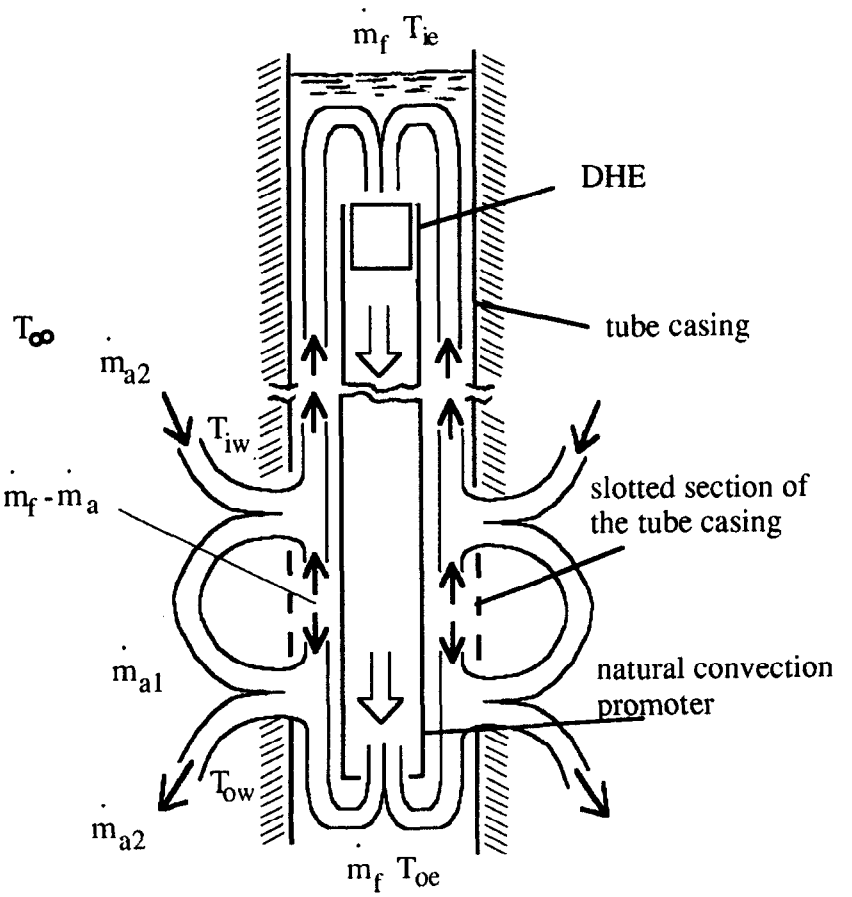

Fig. 5. Sketch of the lumped thermal and flow model of the DHE with annular convection model.

The energy balances (adiabatic mixings) of: (i) the well input renewed geothermal fluid and (ii) the geothermal fluid on the slotted section are, respectively:

$$\dot{m}_{a2}c_p T_\infty + \dot{m}_{a1}c_p T_{ow} = \dot{m}_a c_p T_{iw} \tag{5}$$

case (a) $\dot{m}_a < \dot{m}_f$ [$\delta < 1$, Fig. 4(a)] we can assume that $T_{ow} = T_{oe}$

$$c_p\dot{m}_a T_{iw} + c_p(\dot{m}_f - \dot{m}_a)T_{oe} = c_p\dot{m}_f T_{ie} \tag{6}$$

case (b) $\dot{m}_a > \dot{m}_f$ [$\delta > 1$, Fig. 4(b)] we can assume that $T_{iw} = T_{ie}$

$$c_p\dot{m}_f T_{oe} + c_p(\dot{m}_a - \dot{m}_f)T_{iw} = c_p\dot{m}_a T_{ow}. \tag{7}$$

Moreover the energy balance of the geothermal fluid in: (i) the DHE; (ii) the complete slotted section and (iii) the aquifer-well control volume are, respectively:

$$\dot{Q} = \dot{m}_f c_p(T_{ie} - T_{oe}) \tag{8}$$

$$\dot{Q} = \dot{m}_a c_p(T_{iw} - T_{ow}) \tag{9}$$

$$\dot{Q} = \dot{m}_{a2}c_p(T_\infty - T_{ow}). \tag{10}$$

The momentum equations are then reported in an unusual form. They were obtained by considering that the fluid driving forces are equal to the friction losses only from viscous effects and that these driving forces are directly proportional to the difference of fluid density, the latter being directly proportional to the difference of fluid temperature. Consequently, the momentum equation with lumped parameters on: (i) the slotted section of the tube casing and (ii) and aquifer–well control volume can be expressed, respectively, as:

$$\dot{m}_a c_p = \tau_a(T_\infty - T_{mw}) \tag{11}$$

$$\dot{m}_f c_p = \tau_f(T_{ie} - T_{oe}) \tag{12}$$

where T_{mw} is the mean temperature of the geothermal fluid on the complete slotted section of the tube casing and τ_a and τ_f are parameters characterizing the heat capacity rate for the unit difference of geothermal fluid temperature in the aquifer and in the well, respectively. These parameters are obviously connected to the thermophysical and geometrical parameters of the aquifer (permeability, thermal conductivity, length of the slotted section of the tube casing, etc.).

We can assume that:

$$T_{mw} = T_{ow} + (T_{iw} - T_{ow})\omega \tag{13}$$

where the dimensionless parameter ω is an unknown function of the circulation ratio δ, which meet the following conditions:

$$\text{for } \delta \ll 1 \Rightarrow T_{mw} \cong T_{ow} \tag{14}$$

$$\text{for } \delta \gg 1 \Rightarrow T_{mw} \cong T_{iw}. \tag{15}$$

Consequently, we can assume that ω has the following properties

$$\text{(a)} \begin{cases} \omega = 0 & \text{for } 0 \leqslant \delta \ll 1 \\ \omega = 1/2 & \text{for } \delta = 1 \\ \omega \cong 1 & \text{for } \delta \gg 1 \end{cases}$$

$\omega = f(\delta) \in [0, 1]$ with

$$\text{(b) } \omega' = \frac{df}{d\delta} \geqslant 0 \quad \delta \neq 1. \tag{16}$$

Substituting equation (2) into (5) gives:

$$T_{iw} = \sigma T_{ow} + (1-\sigma)T_\infty \tag{17}$$

from which one obtains:

$$\sigma = \frac{T_\infty - T_{iw}}{T_\infty - T_{ow}} \tag{18}$$

$$1 - \sigma = \frac{T_{iw} - T_{ow}}{T_\infty - T_{ow}}. \tag{19}$$

From equation (19), equation (9) becomes:

$$\dot{Q} = \dot{m}_a c_p(1-\sigma)(T_\infty - T_{ow}). \tag{20}$$

In hypothesis (a) using equation (3), equation (6) can be modified as:

$$T_{ie} = T_{oe} + \delta(T_{iw} - T_{oe}). \tag{21}$$

While in hypothesis (b) using equation (3), equation (7) can be modified as:

$$T_{ow} = T_{iw} - \frac{1}{\delta}(T_{iw} - T_{oe}). \tag{22}$$

Substituting equation (12) into equation (8) we have:

$$\dot{Q} = \frac{(C_p\dot{m}_f)^2}{\tau_f}. \tag{23}$$

Moreover, substituting equation (13) into equation (11) and using equations (9) and (10), we can obtain:

$$\dot{Q} = \frac{\dfrac{(c_p\dot{m}_a)^2}{\tau_a}}{\left(\dfrac{1}{1-\sigma} - \omega\right)}. \tag{24}$$

Equations (5), (23) and (24), and knowledge of functions $\omega(\delta)$ [equation (16)] and $\sigma(\dot{m}_a)$ constitute a nonlinear equation system with six unknowns $\dot{Q}$, $\dot{m}_f$, $\dot{m}_a$, δ, ω and σ; using one as an independent parameter, the remaining five quantities are univocally determined. The model is completed by knowledge of a set of parameters, some of which being imposed as functions of the thermal plant design and some of which being aquifer properties. Among the latter quantities it was noted that parameters τ_f *e* τ_a had to be determined experimentally or by difficult numerical simulation of the aquifer–well–promoter system. Even if their bonds with thermophysical and geometrical characteristics of the aquifer, the well and the promoter are determined, it is even more complex to

determine the function that correlates the various parameters.

By analysing the properties of function ω [see equation (16)] and from equation (24), we can see that $\dot{Q}$ is even more sensitive to variations of σ than of ω. Hence in the present paper the authors have focused their attention to the function $\sigma(\dot{m}_a)$. This function must satisfy the following properties:

$$\text{(a)} \begin{cases} \sigma(0) = 0 \\ \lim_{\dot{m}_a \to \infty} \sigma = 1 \end{cases}$$

$\sigma = \varphi(\dot{m}_a) \in [0, 1]$ with

$$\text{(b)}\ \sigma' = \frac{d\varphi}{d\dot{m}_a} > 0\ \forall\ \dot{m}_a > 0. \tag{25}$$

It should be emphasized that the conditions expressed in equation (25) are not sufficient to demonstrate the existence of a maximum heat flow rate taken from DHE. Hence, in this first phase, by means of a numerical simulation, the authors will determine a number of characteristic values of σ for a number of types of geothermal aquifers and then will determine the function $\sigma(\dot{m}_a)$.

THERMAL AND FLUID DYNAMIC SIMULATION OF A GEOTHERMAL AQUIFER

The thermal and fluid dynamic simulation of a geothermal aquifer was carried out adopting the simplifying hypothesis that the flow induced in the aquifer by a hydraulic gradient is much lower compared to the natural flow that occurs in the aquifer as a result of DHE heat transfer. In this hypothesis, adopting a system of cylindrical coordinates, the thermal and fluid dynamic fields prove to be independent of the angular coordinate. Assuming the Boussinesq approximation, the energy equation and the Darcy's law are [15]:

(1) aquifer

$$\frac{1}{r}\frac{\partial^2\psi}{\partial z^2} + \frac{1}{r}\frac{\partial^2\psi}{\partial r^2} - \frac{1}{r^2}\frac{\partial\psi}{\partial r} = -\frac{kg\beta\gamma}{\mu}\frac{\partial T^*}{\partial r} \tag{26}$$

$$\frac{1}{r}\frac{\partial\psi}{\partial z}\frac{\partial T^*}{\partial r} - \frac{1}{r}\frac{\partial\psi}{\partial r}\frac{\partial T^*}{\partial z} = \frac{\lambda_e}{(\rho c_p)_l}\left(\frac{\partial^2 T^*}{\partial z^2} + \frac{\partial^2 T^*}{\partial r^2} + \frac{1}{r}\frac{\partial T^*}{\partial r}\right) \tag{27}$$

(2) impermeable stratum under aquifer

$$\frac{\partial^2 T^*}{\partial z^2} + \frac{\partial^2 T^*}{\partial r^2} + \frac{1}{r}\frac{\partial T^*}{\partial z^2} = 0 \tag{28}$$

where (i) ψ is the stream function; (ii) $T^* = (T(r, z) - T_{ow})/(T_\infty - T_{ow})$ is the dimensionless temperature; (iii) ρc_p, μ and β are, respectively, the thermal capacity, the dynamic viscosity and the volumetric thermal expansion coefficient of the geothermal fluid; (iv) λ_{eq} is the equivalent thermal conductivity of the aquifer [16]; (v) $\gamma = (T_\infty - T_{ow})$ and (vi) $\boldsymbol{g}$ is the acceleration of gravity. With reference to the geothermal aquifer shown in Fig. 6 the boundary conditions imposed by the numerical simulation are:

thermal boundary conditions

$$T^*(r, z) = 1 \quad \text{for } (r = R \text{ and } 0 \leqslant z \leqslant H_a + H_s) \text{ and } (z = H_a + H_s \text{ and } 0 \leqslant r \leqslant R) \tag{29}$$

$$T^*(r, z) = 0 \quad \text{for } \left(r = r_w \text{ and } \frac{h}{2} \leqslant z \leqslant h\right) \tag{30}$$

$$\frac{\partial T^*(r, z)}{\partial n} = 0 \text{ with } n = z \text{ for } (r_w \leqslant r \leqslant R \text{ and } z = 0) \text{ and } (0 \leqslant r \leqslant r_w \text{ and } z = h) \text{ with } n = r \text{ for } (r = 0 \text{ and } h \leqslant z \leqslant H_a + H_s) \text{ and } \left(r = r_w \text{ and } 0 \leqslant z \leqslant \frac{h}{2}\right) \tag{31}$$

$$T^{*+}(r, z) = T^{*-}(r, z) \quad \text{and} \quad \lambda_s \frac{\partial T^*}{\partial z} = \lambda_{eq} \frac{\partial T^*}{\partial z} \quad \text{for } 0 \leqslant r \leqslant R \text{ and } z = H_a \tag{32}$$

fluid dynamic boundary conditions

$$\frac{\partial\psi(r, z)}{\partial n} = 0 \text{ with } n = r \text{ for } (r_w \leqslant r \leqslant R \text{ and } z = 0) \text{ and } (0 \leqslant r \leqslant r_w \text{ and } z = h) \text{ and for } (0 \leqslant r \leqslant R \text{ and } z = H_a) \text{ with } n = z \text{ for } (r = R \text{ and } 0 \leqslant z \leqslant H_a) \text{ and } (r = 0 \text{ and } h \leqslant z \leqslant H_a) \tag{33}$$

$$\frac{\partial\psi(r, z)}{\partial z} = \left[\frac{2\dot{m}_a}{\pi h}\left(\frac{2z}{h} - 1\right)\right] \text{for } r = r_w \text{ and } 0 \leqslant z \leqslant h \tag{34}$$

where: (i) r_w is the well radius; (ii) h is the height of the slotted section of the tube casing; (iii) R is the size of the geothermal aquifer in which the thermal and fluid dynamic disturbance induced by heat transfer is not felt; (iv) H_a and H_s are the thickness of the geothermal aquifer and of the lower impermeable stratum, respectively; (v) λ_s is the thermal conductivity of the lower impermeable stratum.

The boundary condition (34) imposing that the radial velocity component along the slotted section of the tube casing is a linear function of the height z, was derived in relation to a simple mass exchange model between the well and the aquifer based on the fluid momentum equation, the undisturbed aquifer hydrostatics equation and on the mass transport equation using some simplifying hypothesis; from all these one derives that the renewed mass flow rate at the fluid input is a parabolic function of z.

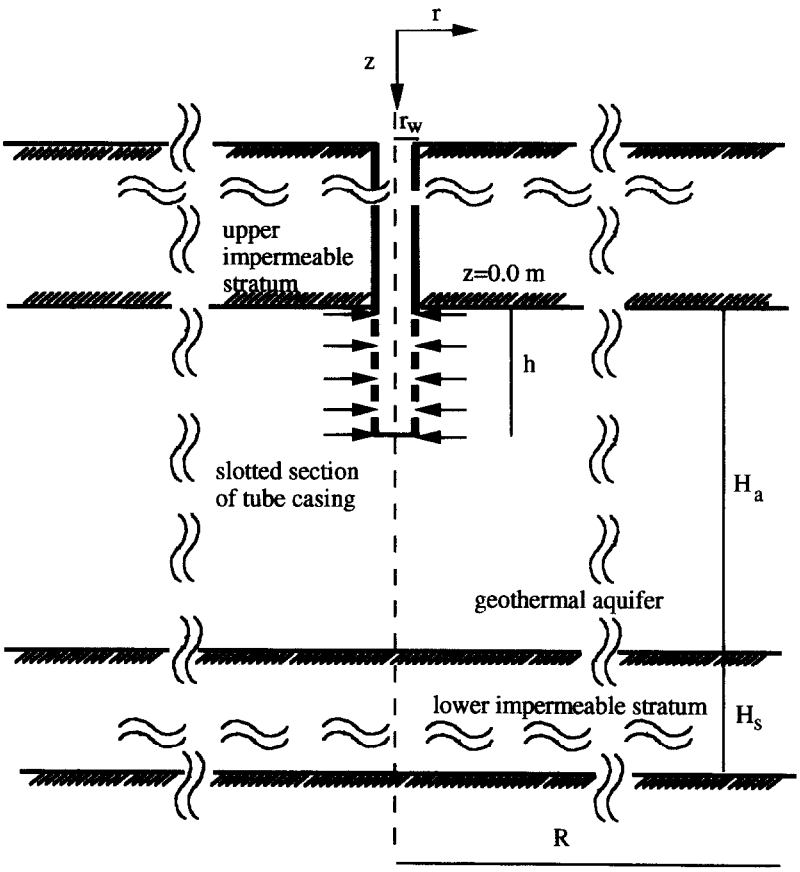

Fig. 6. Layout of geothermal aquifer for thermal and fluid dynamic numerical simulation.

Compared to the numerical simulation discussed in ref. [14], an impermeable soil under the aquifer is considered in the geothermal reservoir scheme. This variation is made in order to identify the influence of boundary conditions on the thermal and fluid dynamic fields. In fact in ref. [14] an adiabatic boundary condition on the bottom of the aquifer were assumed. This boundary condition is realistic only for high aquifer thickness and when the slotted section of the tube casing is positioned immediately below the top of the aquifer. When these conditions are not satisfied the heat transfer from the depth of the geothermal reservoir is not well represented and consequently the heat flow rate withdrawn by the DHE is underestimated. The new scheme with boundary condition expressed by equation (29) taking account that the geothermal reservoir is an infinite heat capacity system compared to the part of the aquifer perturbed by heat flow transferred by the DHE.

Numerical procedure

The system of differential equations (26)–(28), with boundary conditions (29)–(34) were resolved using the finite element method. In particular, to resolve the numerical problem an iterative procedure was applied to determine the thermal and fluid dynamic fields in a separate manner until the solution converges. Assuming that heat and mass flux at the element interfaces are preserved [17], the primary variables (stream function and temperature) can be interpolated with linear functions [18]. A number of isoparametric quadrangular elements were used to discretize the geometrical domain. The mesh is not uniform but a greater number of elements (approximately 600) was used to discretize the domain near the well compared to the remaining part of the aquifer. The number of elements used near the well was in relation to the stability of the thermal and fluid dynamic fields solutions. To estimate the accuracy of the numerical procedure, the exact solutions of one-dimensional and two-dimensional separate thermal and fluid dynamic problems were compared with the corresponding numerical solutions obtaining a maximum percentage error of T and ψ less than 2%.

For high hydraulic conductivity values the iterative method is modified due to convergence problems. In particular, the temperature field used as boundary conditions to solve the fluidodynamic field at the j-iteration, is the average of the temperature values determined at the $(j-1)$ and j-interactions. An analogous scheme for ψ-boundary conditions is used to solve the temperature field at the j-iteration.

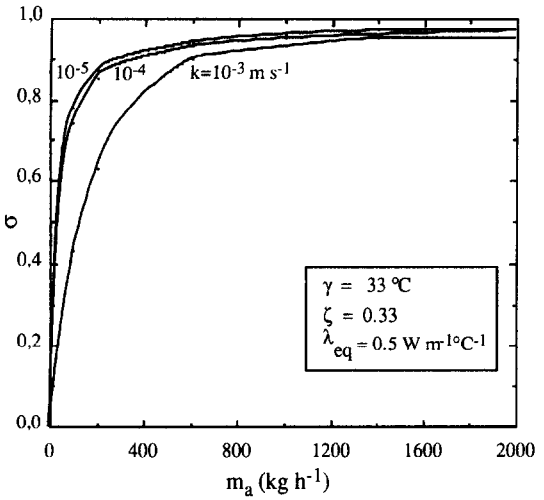

Fig. 7. Short-circuit factor trend vs aquifer hydraulic conductivity variations.

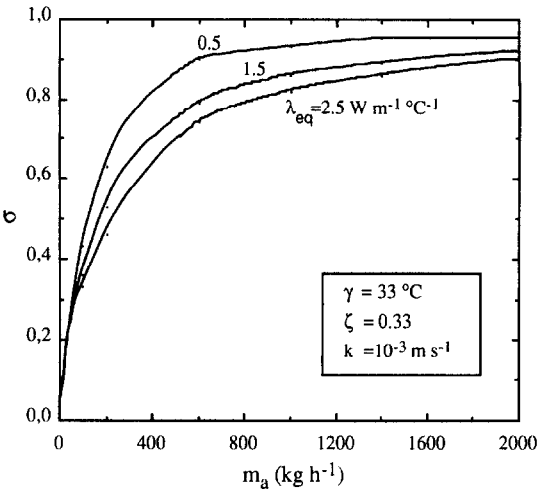

Fig. 8. Short-circuit factor trend vs aquifer equivalent thermal conductivity variations.

In this first phase the numerical simulations carried out were limited to the case of the slotted section of tube casing being positioned beginning from the upper position of the geothermal aquifer. Furthermore, the height of the slotted section of tube casing h and the well radius r_w were maintained constant, respectively at 3 and 0.175 m, the thermal conductivity of the impermeable soil and the equivalent conductivity of the aquifer were supposed to be equal and moreover the impermeable soil thickness under the aquifer was 3 m. The following parameters, instead, were allowed to vary, in the following intervals:

$$0.33 \leqslant \zeta = \frac{h}{H_a} \leqslant 1.0; \quad 13 \leqslant \gamma = T_\infty - T_{ow} \leqslant 33°C;$$

$$50 \leqslant \dot{m}_a \leqslant 2000\,\mathrm{kg\,h^{-1}} \quad 0.5 \leqslant \lambda_{eq} \leqslant 2.5\,\mathrm{W\,m^{-1}\,°C^{-1}}$$

$$10^{-5} \leqslant k \leqslant 10^{-3}\,\mathrm{m\,s^{-1}}. \qquad (35)$$

Determining the field of temperature and the stream function in the aquifer proved the existence of geothermal fluid short-circuiting near the well. Determining the field of temperature, in particular in the upper part of the slotted section of tube casing, allowed the mean geothermal fluid input temperature in the well to be determined as follows:

$$T_{iw} = \frac{2\gamma}{h}\int_{h/2}^{0} T^*(r_w, z)\,dz - T_{ow}. \qquad (36)$$

Substituting the value obtained from equation (36) in equation (18) we can determine the value of the geothermal fluid short circuit factor for each case of the numerical simulation.

Results

Some of the most significant results obtained through numerical simulation are shown in Figs. 7–10. As reported in ref. [14] from these diagrams it can be seen that the short circuit factor σ trend is shown as a function of the renewed fluid mass flow rate as the characteristic aquifer parameters vary. In these figures the short circuit factor tends asymptotically towards unity when the renewal fluid mass flow rate increases. This verifies the hypothesis that $T_{iw} \neq T_\infty$ on the basis of the model proposed by the authors.

From Figs. 7–10 it can be seen that the short circuit factor σ:

(i) Increases as the hydraulic conductivity of the aquifer, k, diminishes (Fig. 7). In fact, for every other parameter, and in particular for $\dot{m}_a$ being equal, the decrease in k gives rise to an increase in geothermal fluid velocity with a consequent increase in the short circuit effect.

(ii) Increases as the equivalent thermal conductivity of the aquifer, λ_{eq}, diminishes (Fig. 8). In fact, for every other parameter being equal, the

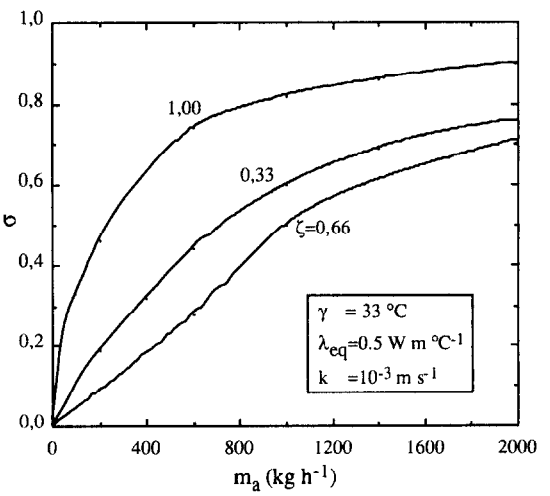

Fig. 9. Short-circuit trend vs the ratio between the height of the slotted section of tube casing and the aquifer thickness.

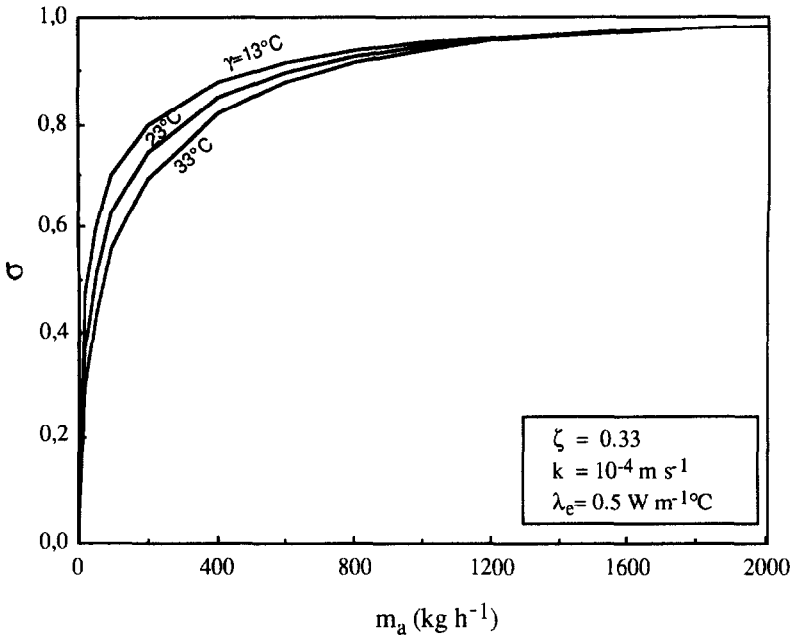

Fig. 10. Short-circuit factor trend vs variations in the output temperature of well geothermal fluid.

decrease in λ_{eq} determines a decrease in aquifer heat transfer with a consequent decrease in the temperature of the geothermal fluid input to the well, T_{iw}, and, therefore, of the short circuit factor

(iii) Increases as the dimensionless thickness of the aquifer ζ tends to one (Fig. 9), since elevations of z geometrically tie the convective cell extension induced by the removal of energy, thereby increasing the resistance to movement of the renewed fluid and favouring short circuit formation. ζ also increases when it tends to low values. This depends to the high distance of the slotted section of the tube casing from the zone of the heat transfer from the depth of the geothermal reservoir. Consequently, the slotted section position is very important to optimize the design of DHE, and this position is a function of the thickness of the aquifer. Specified studies must be carried out to investigate this problem.

(iv) Increases as the output temperature T_{ow} of the geothermal fluid from the slotted section of tube casing increases (Fig. 10). The influence of this parameter can to a good approximation be considered as being negligible.

We also want to underline that if the numerical procedure is the same as that reported in Ref. [14], the results are different, since (i) the simulation scheme of the geothermal reservoir is different; (ii) the heat and mass flows are greater, and so consequently a wider range of $\dot{m}_a$ is considered.

Comparing the numerical results of σ obtained using the adiabatic boundary condition on the bottom of the aquifer reported in ref. [14] with the results determined considering the impermeable soil under the aquifer, it is evident that the values of σ in the first case are less than the corresponding values of the second case for low aquifer thickness, whereas for high thicknesses the values are practically equal.

As reported in ref. [14], the results of σ obtained by numerical simulations were interpolated as a function of $\dot{m}_a$ by means of the minimum square technique, thereby obtaining the following relationship for all examined conditions of the aquifer that were characterized by the combination of H_a, λ_{eq}, T_{ow} and k:

$$\sigma = 1 - \exp[-a(c_{pl}m_a)^b]. \quad (37)$$

Equation (37) allows σ to be determined in the interval defined by equation (35) with a maximum error of 2%. Now we want to emphasize that the function $\sigma(\dot{m}_a)$ expressed by equation (37) determines a maximum value of heat flow rate [see equation (19)] as discovered experimentally by the authors.

A trend of the values of the dimensional coefficients a and b are given in Fig. 11 as the hydraulic permeability varies and for a characteristic set of ζ, λ_{eq}, γ. From this figure it can be seen that the trend of coefficients a and b can be assumed to be almost linear and in particular, coefficient b is almost constant as k varies and is independent of the value of equivalent thermal conductivity. Tables 1–3 show some values of a and b for some combinations of ζ, λ_{eq}, γ and k. Analogous values for the case of the aquifer with the adiabatic boundary condition on the bottom of the aquifer are reported in ref. [14].

Substituting equation (37) into equation (20) one obtains:

$$\dot{Q} = \dot{m}_a c_p \exp[-a(c_p\dot{m}_a)^b](T_\infty - T_{ow}) \quad (38)$$

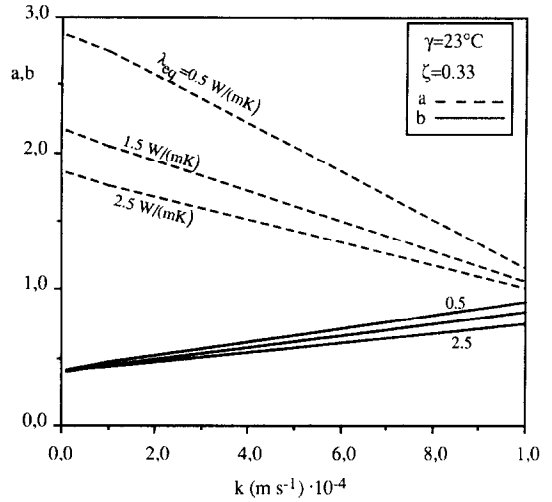

Fig. 11. Values of a and b coefficients vs aquifer permeability variations.

deriving the same equations to $\dot{m}_a$ and making it equal to zero. Expressing equation (38) for Q_{max}, one can obtain:

$$c_p \dot{m}_{a(\dot{Q}_{max})} = (ab)^{-1/b} \tag{39}$$

where $\dot{m}_{a(\dot{Q}_{max})}$ is the renewed geothermal fluid rate corresponding to the heat flow rate transferred by the DHE.

Introducing the dimensionless parameters:

$$\chi = \frac{\dot{Q}}{Q_{max}} \quad \xi = \frac{\dot{m}_a}{\dot{m}_{a(\dot{Q}_{max})}} \tag{40}$$

and substituting equation (40) into equation (39) we obtain

$$\chi = \xi \exp\left[-\frac{(\xi^b - 1)}{b}\right]. \tag{41}$$

Figure 12 shows the values of χ as ξ varies for a number of values of b. It can be seen from this diagram

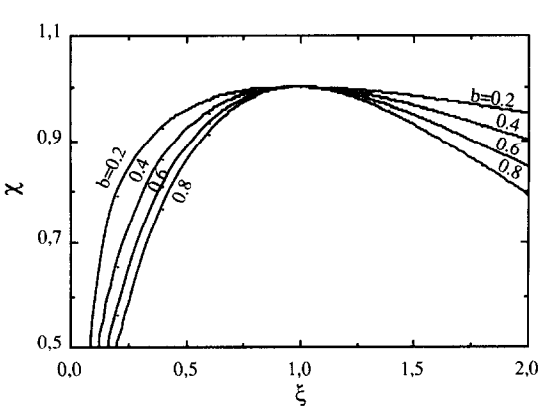

Fig. 12. $\chi = \dot{Q}/\dot{Q}_{max}$ trend vs $\xi = \dot{m}_a/\dot{m}_{a(\dot{Q}_{max})}$ as a function of parameter b.

that the function $\chi(\xi)$ does not increase monotonically but is at a maximum. Hence, as $\dot{m}_a$ increases beyond the value corresponding to this maximum, the heat flow rate transferred by the DHE tends to diminish, in accordance with the experimental findings of the Ischia plant where $\dot{Q}$ diminished as T_{ic} diminished. It is evident, however, that within the well temperature is interconnected and therefore as T_{ic} diminishes, there is a corresponding decrease in the temperature of the geothermal fluid at the input of the evaporator tube bundle T_{iw} and at the output of the slotted section of tube casing T_{ow}.

Comparing the numerical results obtained using the adiabatic boundary condition on the bottom of the aquifer reported in ref. [14] with the results determined considering the impermeable soil under the aquifer, it is evident that the maximum heat flow transferred by the DHE in the first case is less than the corresponding values of the second case for low aquifer thickness, whereas for high thicknesses the values are practically equal.

CONCLUSIONS

In their study the authors have verified both experimentally, and by means of numerical simulation, that the heat flow rate that can be transferred from a geothermal aquifer by a DHE with a natural convection promoter are tied to a maximum value. The presence of this maximum value depends on a short circuit effect in the flow of the geothermal fluid that occurs near the slotted section of tube casing. In order to consider this effect in the heat and mass transfer, the authors developed a simplified thermal and fluid dynamic model with lumped parameters to design a DHE with a natural convection promoter. In this model the authors introduced some characteristic parameters of the aquifer–well–promoter system. In particular, in this paper they examined the most significant parameter defined as the short-circuit factor. This factor is a function of (i) the aquifer and the well geometrical characteristics; (ii) the permeability and equivalent thermal conductivity of the aquifer; and (iii) the difference in temperature between the unperturbed aquifer and the temperature of the geothermal fluid downstream of the heat transfer. Some short circuit factor values were obtained by the authors for variations of the above-mentioned parameters by means of a numerical simulation of a geothermal aquifer using the finite element method.

The numerical simulation and the experimental tests carried out on particular type of DHE have allowed the authors to understand that the maximum value of DHE is a function of the characteristics of the thermal plant, the aquifer and the well configuration and, in particular, of the dimensions and position in the aquifer of the slotted section of tube casing, and the natural convection promoter.

Table 1. Dimensional coefficients a and b for a characteristic set of k, λ_{eq}, γ and $\zeta = 1.0$

	$\zeta = 1.00$								
	$\gamma = 33°C$			$\gamma = 23°C$			$\gamma = 13°C$		
	$\lambda_{eq} = 0.5$ W m^{-1} K^{-1}	$\lambda_{eq} = 1.5$ W m^{-1} K^{-1}	$\lambda_{eq} = 2.5$ W m^{-1} K^{-1}	$\lambda_{eq} = 0.5$ W m^{-1} K^{-1}	$\lambda_{eq} = 1.5$ W m^{-1} K^{-1}	$\lambda_{eq} = 2.5$ W m^{-1} K^{-1}	$\lambda_{eq} = 0.5$ W m^{-1} K^{-1}	$\lambda_{eq} = 1.5$ W m^{-1} K^{-1}	$\lambda_{eq} = 2.5$ W m^{-1} K^{-1}
$k = 10^{-5}$ m s^{-1}	$a = 3.27$ $b = 0.363$	$a = 2.346$ $b = 0.446$	$a = 1.88$ $b = 0.428$	$a = 3.35$ $b = 0.373$	$a = 2.37$ $b = 0.430$	$a = 1.88$ $b = 0.428$	$a = 3.18$ $b = 0.340$	$a = 2.26$ $b = 0.411$	$a = 2.02$ $b = 0.450$
$k = 10^{-4}$ m s^{-1}	$a = 3.09$ $b = 0.387$	$a = 2.19$ $b = 0.452$	$a = 2.22$ $b = 0.547$	$a = 3.09$ $b = 0.385$	$a = 2.22$ $b = 0.435$	$a = 1.86$ $b = 0.445$	$a = 3.16$ $b = 0.376$	$a = 2.28$ $b = 0.435$	$a = 1.87$ $b = 0.446$
$k = 10^{-3}$ m s^{-1}	$a = 2.24$ $b = 0.363$	$a = 1.78$ $b = 0.613$	$a = 1.55$ $b = 0.604$	$a = 2.50$ $b = 0.576$	$a = 1.91$ $b = 0.591$	$a = 1.62$ $b = 0.571$	$a = 2.94$ $b = 0.547$	$a = 2.064$ $b = 0.541$	$a = 1.711$ $b = 0.532$

Table 2. Dimensional coefficients a and b for a characteristic set of k, λ_{eq}, γ and $\zeta = 0.66$

	$\zeta = 0.66$								
	$\gamma = 33°C$			$\gamma = 23°C$			$\gamma = 13°C$		
	$\lambda_{eq} = 0.5$ W m^{-1} K^{-1}	$\lambda_{eq} = 1.5$ W m^{-1} K^{-1}	$\lambda_{eq} = 2.5$ W m^{-1} K^{-1}	$\lambda_{eq} = 0.5$ W m^{-1} K^{-1}	$\lambda_{eq} = 1.5$ W m^{-1} K^{-1}	$\lambda_{eq} = 2.5$ W m^{-1} K^{-1}	$\lambda_{eq} = 0.5$ W m^{-1} K^{-1}	$\lambda_{eq} = 1.5$ W m^{-1} K^{-1}	$\lambda_{eq} = 2.5$ W m^{-1} K^{-1}
$k = 10^{-5}$ m s^{-1}	$a = 2.41$ $b = 0.288$	$a = 1.82$ $b = 0.409$	$a = 1.50$ $b = 0.447$	$a = 2.40$ $b = 0.310$	$a = 1.71$ $b = 0.418$	$a = 1.43$ $b = 0.474$	$a = 2.22$ $b = 0.333$	$a = 1.55$ $b = 0.447$	$a = 1.24$ $b = 0.552$
$k = 10^{-4}$ m s^{-1}	$a = 2.09$ $b = 0.533$	$a = 1.60$ $b = 0.511$	$a = 1.36$ $b = 0.509$	$a = 2.05$ $b = 0.473$	$a = 1.55$ $b = 0.507$	$a = 1.32$ $b = 0.530$	$a = 1.97$ $b = 0.466$	$a = 1.43$ $b = 0.556$	$a = 1.16$ $b = 0.610$
$k = 10^{-3}$ m s^{-1}	$a = 0.760$ $b = 0.760$	$a = 0.606$ $b = 0.843$	$a = 0.545$ $b = 0.865$	$a = 0.853$ $b = 0.595$	$a = 0.680$ $b = 0.782$	$a = 0.614$ $b = 0.788$	$a = 0.948$ $b = 0.638$	$a = 0.708$ $b = 0.735$	$a = 0.649$ $a = 0.788$

Table 3. Dimensional coefficients a and b for a characteristic set of k, λ_{eq}, γ and $\zeta = 0.33$

	$\zeta = 0.33$								
	$\gamma = 33°C$			$\gamma = 23°C$			$\gamma = 13°C$		
	$\lambda_{eq} = 0.5$ W m^{-1} K^{-1}	$\lambda_{eq} = 1.5$ W m^{-1} K^{-1}	$\lambda_{eq} = 2.5$ W m^{-1} K^{-1}	$\lambda_{eq} = 0.5$ W m^{-1} K^{-1}	$\lambda_{eq} = 1.5$ W m^{-1} K^{-1}	$\lambda_{eq} = 2.5$ W m^{-1} K^{-1}	$\lambda_{eq} = 0.5$ W m^{-1} K^{-1}	$\lambda_{eq} = 1.5$ W m^{-1} K^{-1}	$\lambda_{eq} = 2.5$ W m^{-1} K^{-1}
$k = 10^{-5}$ m s^{-1}	$a = 2.86$ $b = 0.325$	$a = 2.17$ $b = 0.398$	$a = 1.83$ $b = 0.412$	$a = 2.87$ $b = 0.323$	$a = 2.17$ $b = 0.398$	$a = 1.85$ $b = 0.416$	$a = 3.20$ $b = 0.371$	$a = 2.16$ $b = 0.391$	$a = 1.70$ $b = 0.374$
$k = 10^{-4}$ m s^{-1}	$a = 2.02$ $b = 0.471$	$a = 1.96$ $b = 0.462$	$a = 1.71$ $b = 0.451$	$a = 2.75$ $b = 0.475$	$a = 2.05$ $b = 0.442$	$a = 1.75$ $b = 0.441$	$a = 2.84$ $b = 0.395$	$a = 2.13$ $b = 0.426$	$a = 1.79$ $b = 0.426$
$k = 10^{-3}$ m s^{-1}	$a = 0.939$ $b = 0.648$	$a = 0.787$ $b = 0.855$	$a = 0.787$ $b = 0.855$	$a = 1.15$ $b = 0.904$	$a = 1.05$ $b = 0.835$	$a = 1.00$ $b = 0.753$	$a = 1.46$ $b = 0.195$	$a = 1.44$ $b = 0.687$	$a = 1.27$ $b = 0.180$

REFERENCES

1. Culver, G. and Reistad, G. M., Testing and modelling of downhole heat exchanger in shallow system. *Geothermal Resources Council Transaction*, 1978, **2**, 129–131.
2. Horner, R. N., Design considerations of a downhole coaxial geothermal heat exchanger. *Geothermal Resources Council Transaction*, 1980, **4**, 569–572.
3. Allis, R. G., A study of the use of downhole heat exchanger in the Moana hot water area, Reno. *Geo-Heat Center Report*, Oregon Institute of Technology, 1980.
4. Morita, K., Matsubajashi, O. and Kusunoki, K., Downhole coaxial heat exchanger using insulated inner pipe for maximum heat extraction. *Geothermal Resources Council Transaction*, 1985, **9**, 45–49.
5. Culver, G., Downhole heat exchangers. *Geo-Heat Center Bulletin*, 1989, **11**(3), 1–4.
6. Culver, G., Downhole heat exchangers. *Geo-Heat Center Report*, Oregon Institute of Technology, 1990.
7. Kreitlow, D. B., Reistad, G. M., Miles, C. R. and Culver, G. G., Thermosyphon models for downhole exchanger applications in shallow geothermal system. *Journal of Heat Transfer*, 1978, **100**, 713–719.
8. Allis, R. G. and James, R. C., A natural convection promoter for geothermal wells. *Geothermal Resourcers Council Transaction*, 1980, **4**, 409–412.
9. Cannaviello, M., Casarosa, C., Latrofa, E., Martorano, L. and Reale, F., Gravity heat pipe as geothermal convectors. In *Advances in Heat Pipe Technology*. Pergamon Press, Oxford, 1982, pp. 759–776.
10. Cannaviello, M., Carotenuto, A., Casarosa, C., Latrofa, E., Martorano, L. and Reale, F., An advanced system for heat transfer from geothermal low and medium enthalpy sources. *Proceedings of the Conference on Geothermal Energy*, Vol. 2, Firenze, 1982, pp. 63–80.
11. Casarosa, C. and Dobran, F., Experimental investigations and analytical modelling of a closed two-phase thermosyphon with imposed convection boundary conditions. *International Journal of Heat and Mass Transfer*, 1988, **31**, 1815–1833.
12. Latrofa, E., Casarosa, C., Martorano, L., Cannaviello, M. and Carotenuto, A., Geothermal convector design: solutions, design criteria, calculation methods. *Energy Source*, 1994, **16**, 531–547.
13. Carotenuto, A., Casarosa, C. and Martorano, L., The geothermal convector: experimental results. *Proceedings of the National Reference of the Conference of the ATI*, Vol. 1, Parma, 1992, pp. 27–45. Submitted to *Journal of Heat Transfer, ASME*, 1997.
14. Buonanno, G., Carotenuto, A., Casarosa, C. and Martorano, L., An aquifer–well thermofluidodynamic model to design a downhole heat exchanger. *Proceedings of an International Conference on Porous Media and its Applications in Science, Engineering and Industry*, Kona, Hawaii, 1996, pp. 532–553.
15. Cheng, P., Geothermal heat transfer. In *Handbook of Heat Transfer*, 2nd edn, ed. W. M. Rohsenow, J. P. Hartnett and E. Ganic. McGraw-Hill, New York, 1985.
16. Nozad, I., Carbonell, R. G. and Whitaker, S., Heat conduction in multiphase systems—I: theory and experiment for two-phase systems. *International Journal of Heat and Mass Transfer*, 1985, **40**(5), 843–855.
17. Patankar, S. V., *Numerical Heat Transfer and Fluid Flow*. McGraw-Hill, New York, 1980.
18. Reddy, J. N., *An Introduction to the Finite Element Method*. McGraw-Hill, New York, 1984.